Predicting the Electrokinetic Properties on an Outcrop and Reservoir Composite Carbonate Surfaces in Modified Salinity Brines using Extended Surface Complexation Models

Joel T. Tetteh[1,2*], Anthony Pham[2], Edward Peltier[2], Justin M. Hutchison,[2] and Reza Barati Ghahfarokhi[1,3]

[1]Chemical and Petroleum Engineering Department, University of Kansas

[2]Civil, Environmental, and Architectural Engineering Department, University of Kansas

[3]Tertiary Oil Recovery Program, University of Kansas

[*]Correspondence to: Joel T. Tetteh (Email: joelteyetetteh@gmail.com)

Abstract

Surface complexation models (SCM), based mainly on the diffuse double layer (DDL) theory, have been used to predict zeta potential at the crude oil-brine-rock (COBR) interface with limited success. However, DDL is inherently limited in accurately predicting zeta potential by the assumptions that all the brine ions interact with the rock surface at the same plane and by the double layer collapse at higher brine ionic strength (> 1M). In this work, a TLM-based SCM captured zeta potential trends at the calcite-brine interface with ionic strength up to 3M. An extended DDL and TLM-based SCMs were used to predict the electrokinetic properties of a composite carbonate rock showing a different mineralogical composition. The extended TLM-based SCM captured the zeta potential prediction trends and magnitude, highlighting the contribution of the inorganic minerals and organic impurities on the composite carbonate surface. In contrast, the extended DDL-based SCM captured the zeta potential trends but failed to capture the magnitude of the measured zeta potential. Interestingly, the TLM-based SCM predicted a positive SP for the rock-brine interface, which could explain the oil-wet nature of composite carbonate rocks due to electrostatic adsorption of negatively charged carboxylic acids. Conversely, the DDL-based SCM predicted a negative SP, leading to an inaccurate interpretation of the electrokinetic properties at the rock-brine interface. Thus, the use of extended TLM-based SCM was required to accurately predict the zeta potential and account for the adsorption of carboxylic acids on the reservoir composite carbonate surface.

1. Introduction

Carbonate rocks contain approximately 60% of hydrocarbon reserves in the world [1, 2]. However, only about 30% of the oil is recovered from these carbonate formations due to their oil-wet nature [3]. Carbonate rock surfaces exhibit positive potential below pH 8-9 [4], while a typical crude oil surface exhibits a negative potential at pH above 3-5 [5, 6]. These oppositely charged surfaces promote electrostatic attraction and limit oil extraction [4, 7]. The presence of brines also affects the wettability state of the carbonates. Rock wettability is dependent on the electrostatic surface potential (SP) of the oil-brine and the rock-brine interface [5, 8].

The adsorption of potential determining ions (PDIs, which include SO_4^{2-}, Mg^{2+}, Ca^{2+}, and CO_3^{2-}) and the reduction of brine salinity can alter the carbonate wettability state towards intermediate to water-wetness, resulting in improved oil recovery [9-14]. Thus, water chemistry is an important parameter influencing carbonate rock wettability [15-17]. Jackson et al. [10] observed that the same zeta potential at the rock-brine and the oil-brine interface was needed to trigger the wettability alteration responsible for improved oil recovery observed in carbonates. Mahani et al. [11-13] also observed that increased SO_4^{2-} adsorption and reduced brine salinity triggered a negative zeta potential on limestone surface, which would generate a repulsive disjoining pressure leading to wettability alteration. In a similar observation in chalk, Zhang et al. [17, 18] suggested that increased SO_4^{2-} and decreased Ca^{2+} concentrations would generate a negative zeta potential at the chalk-brine interface. This would alter the surface wettability towards water wetness through multivalent ionic exchange and hence improve oil recovery. Mg^{2+} was later observed to be more active at the chalk surface than Ca^{2+} at higher temperatures (above 110^{o}C) and hence would greatly impact the measured zeta potential [19]. Thus, the concentration of SO_4^{2-}, Ca^{2+}, Mg^{2+} and lower brine salinity can all preferentially alter the surface potential and rock wettability, and improve oil recovery in carbonates.

Carbonate rock mineralogy has also been observed to influence surface electrokinetics. It is widely known that limestone rock is mainly made up of calcite mineral. However, reservoir-based limestone rocks

also include other minerals such as dolomite, anhydrite, and quartz and can be covered in organic matter (OM). As such, these rocks could be referred to as composite carbonate rocks [20-22]. Due to the exposure of reservoir carbonates to crude oil molecules during migration and storage, OM adsorption on the rock surface could also be expected. Vdovic [23] observed that naturally occurring limestone rock returned a negative zeta potential in a 10^{-3} M NaCl solution as compared to the positive zeta potential returned by synthetic calcite in the same aqueous solution. Other researchers have also observed differences between measured zeta potential of natural and synthetic carbonates [22, 24]. These observations were attributed to the presence of organic impurities attached to the surface or incorporated in the structure of the calcite.

Surface complexation modeling (SCM) has recently emerged as a technique to characterize the electrostatic interactions at the rock-brine interface [8, 9, 22, 25-32]. These efforts have focused on accounting for the influences of water chemistry and rock mineralogy. Electrokinetic properties of carbonate rocks are mostly determined using synthetic calcite powder or outcrop limestone powder with high calcite composition (≥99%). Therefore, it is prudent to represent the electrokinetic interaction using a pure calcite surface. Calcite mineral is known to have the capability to behave as a charged colloidal particle when dispersed in aqueous solutions [33, 34]. Brady and Thyne [8] illustrated the adsorption of PDIs on the carbonate surfaces using analogous geochemical reactions and constants from the literature. They coupled the SCM with a transport model to characterize the role of surface species on the wettability and predict additional oil recovery in limestone rock from experimental data by Yousef et al. [35]. Tetteh et al. [9, 25] later modified the reaction constants from the SCM by Brady and Thyne [8] to match the zeta potential of the limestone surface using brines of different salinity and ionic composition. This approach successfully predicted the wettability state on the limestone surface by highlighting the electrostatic bond linkages formed between the species on the rock-brine and the oil-brine interface [9, 25]. Similar use of SCM to characterize carbonate surface and wettability alteration has been performed in the literature [26, 29, 30, 36, 37]. Song et al [22], observed that an SCM developed on a pure calcite surface was insufficient to predict zeta potential of complex reservoir limestone rocks. In an attempt to correct for the discrepancy,

Song et al [22] incorporated inorganic silica to represent quartz compositions and organic impurities onto the limestone surface but ignored the presence of dolomite mineral, which was assumed to react similarly to calcite. However, dolomite and calcite surfaces react differently with brine [38], which could impact the electrokinetic properties on a carbonate rock with significant dolomite compositions.

The diffused double layer (DDL)-based SCM is the most common approach used to capture the electrokinetic properties of a calcite surface and predict carbonate rock wettability [8, 9, 25, 28-32, 37, 39, 40]. **Figure 1** shows the description of the interaction of ions with the calcite interface in the electrical double layer (EDL) using the DDL and TLM-based SCM. The DDL-based SCM assumes that the adsorption of the PDIs and the indifferent ions (Na^+, K^+, and Cl^-) occurs at the hydrolysis layer, with the counter ions located in the diffused layer, thus making it simpler and easier to execute [41-43] (**Figure 1**A). However, the interaction of the ions towards the calcite surface is different. Stipp (1991) [44] used X-ray photoelectron spectroscopy to indicate the presence of the hydrolysis layer, which results in the adsorption of the H and OH ions onto the calcite surface to form >CaOH and $>CO_3H$ primary hydration sites [32, 33, 44, 45]. Stipp 1991 [44] also identified Ca^{2+} and CO_3^{2-} as PDIs that absorb to the calcite surface. Later, Al Mohrouqi et al [45], identified these PDIs as adsorbing onto the calcite lattice at the inner Helmholtz plane (IHP). In recent years, Mg^{2+}, and SO_4^{2-} ions have also been identified as PDIs at the calcite surface through different geochemical interaction experiments [16, 18, 19]. Thus, these ions could be assumed to adsorb onto the calcite surface at the IHP. The hydrated molecules associated with PDIs would stay at the Stern layer due to the larger molecule diameter, while the indifferent ions stay in the diffused layer to provide charge balance at the calcite surface. Therefore, the use of the DDL model may not accurately capture the ionic interactions at the calcite lattice.

The DDL-based SCM calculates the zeta potential from the Debye-Hückel approximation of the Poisson-Boltzman Equation for zeta potential $\leq \pm 25$mV [46, 47]. The Debye-Hückel approximation was also developed for 1:1 symmetrical electrolyte solution and hence could result in inaccuracies when used for multi-ion salt solutions. [46, 47]. On the other hand, a triple layer model (TLM), a type of SCM, can

be used to correctly place the ionic interactions at the right planes within the Stern and the diffuse layer (**Figure 1**B) by assuming spatial distribution of the ions in the different planes. The potential is assumed to linearly drop from the surface to the IHP and then to the outer Helmholtz plane (OHP) at the end of the stern layer based on different capacitance between the three parallel planes. By this approach, the concentration of the surface species could be correctly calculated, and their role in influencing the wettability state of carbonates could be rightly stated. Furthermore, the potential at the OHP could be assumed as the zeta potential and matched to experimental data to avoid the use of the Debye-Hückel approximation. Even though the TLM is more accurate in predicting the electrostatic interactions at the rock-brine interface, it has been used very sparingly to characterize calcite-brine interfaces [26, 27, 36].

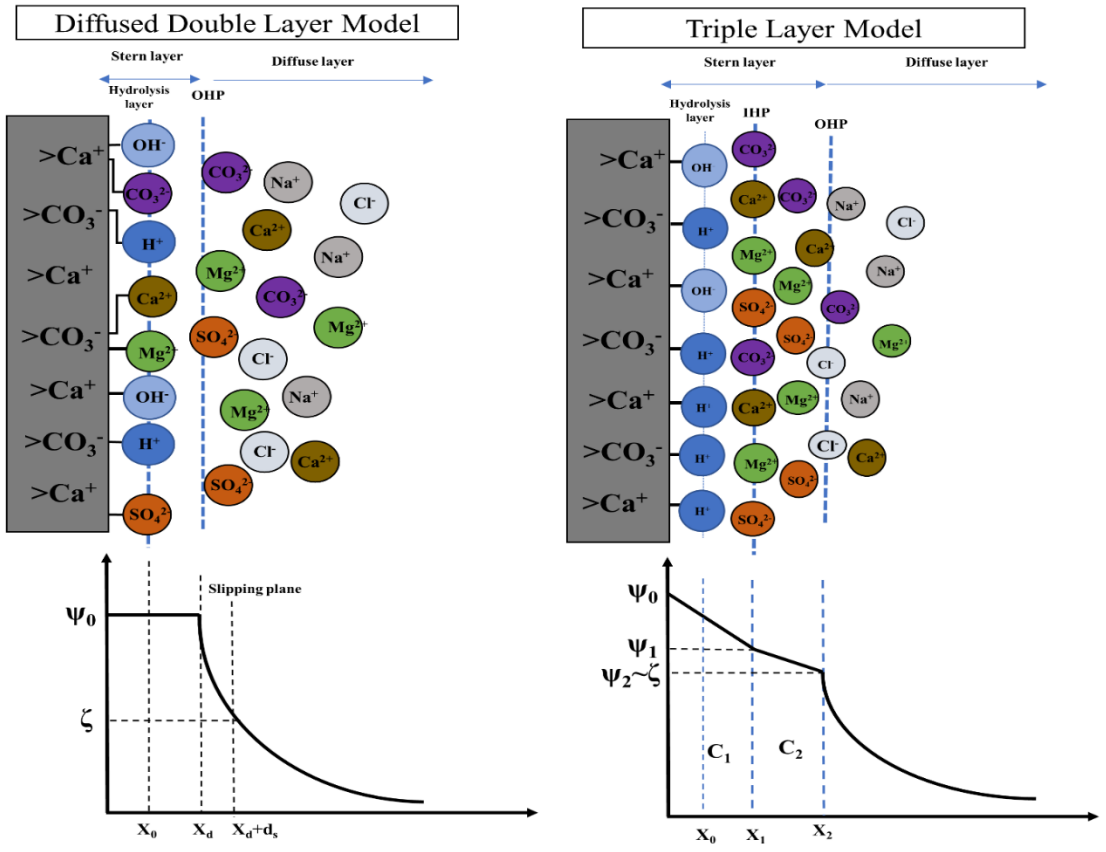

Figure 1: Schematic description of the diffused double layer (DDL) model (left) and the Triple layer model (TLM, right) of a pure calcite surface. The calcite surface is made up of Ca^{2+} and CO_3^- reactive sites, which interacts with H^+ and OH^- to form the $>CO_3H$ and the $>CaOH$ primary hydration sites. For the DDL model, ions are assumed to interact with the Ca^{2+} and CO_3^- reactive sites to form different species at the hydrolysis layer (X_0), representative of the calcite surface. For the TLM, ions interact with the calcite surface at different planes based on the understanding of the geochemical of calcite-brine interfaces. Refer to [32, 41, 45, 48] for more details.

This work compared both DDL and TLM-based SCMs to predict different zeta potential trends and electrostatic interactions at the calcite-brine interface when using real-world produced water brines. The adsorption of PDIs on the calcite-brine interface was examined using both models to elucidate the effect of correctly placing PDIs in the appropriate planes. To account for the real-world composition of a reservoir composite carbonate surfaces, extended DDL- and TLM-based SCMs were also developed by incorporating dolomite, quartz, and organic impurities onto the calcite lattice. This would enable electrostatic characterization and prediction of the electrokinetic properties of composite carbonate surface, elucidating their contribution and roles in determining the wettability of composite carbonate rock. To the best of the authors' knowledge, accurately modeling the electrostatic interactions and predicting electrokinetic properties between real-world PW and a reservoir carbonate surface using the TLM has not been previously reported.

2. Materials and Methods

2.1. Rocks

Two carbonate core samples were used for the zeta potential measurements and assessment of the SCMs. Outcrop Indiana limestone rock purchased from Kocerek Industry represents pure calcite surface, as it is composed of 99% calcite [9, 25, 49]. Reservoir composite carbonate rock from the Lansing Kansas City (LKC) formation in the Central Kansas Uplift was acquired from an oil-producing well in Haskell County. XRD analysis was performed on the powdery rock samples as previously described [49]. **Table 1** shows the mineralogical composition of the rocks used.

Table 1: XRD analysis of carbonate rock used (% w/w)

	Calcite	Dolomite	Quartz
Indiana Limestone	≥99	trace	trace
Lansing Kansas City (LKC) carbonate	84.9	11.7	3.4

2.2. Brine Preparation and Characterization

PW brine and synthetic formation water salinity (FWS) brines were used in the zeta potential analysis, with ACS-grade chemicals (Fisher Scientific) used to create synthetic brines. PW samples were acquired from the Arbuckle formation in the Central Kansas Uplift. These samples were taken from the wellhead before application of any separation chemicals to preserve the chemical composition of the PW. PW samples were vacuum filtered using a 0.45-micron PVDF filter to remove any solids present. Initial pH measurements of the brines were obtained using a LAQUAtwin–pH 22 compact pH meter.The concentrations of dissolved cation species (Ba, K, Fe, Mn, Mg, Al, Sr, Li, Ca, and Na) were measured using inductively coupled plasma–optical emission spectrometry (ICP–OES) (Optima 2000 DV instrument, PerkinElmer). The samples were diluted as necessary to meet the analytical range and preserved by adding concentrated nitric acid to create 2% (v/v) solutions prior to analysis. Ion chromatography (IC) (Dionex Integrion HPIC with Dioinex IonPac AS18 column) was used to determine concentration of anionic species (Cl^-, NO_2^-, SO_4^{-2}, Br^-, and NO_3^-) , again with appropriate dilution to reach the analytical range of the instrument. Milli-Q water (18.2 MΩ) was used for all brine dilutions.

A synthetic FWS brine (ionic strength of 3.27 M), with a composition similar to brines from the Trembley range field in Kansas (data provided by the operator), was prepared by adding different amounts of NaCl, KCl, $MgCl_2.6H_2O$, $CaCl_2.2H_2O$, and Na_2SO_4 to deionized water. Seawater-like salinity brine (SWS) and low salinity brine (LSW) were prepared by diluting the FWS by a factor of five (5) and eighty-two (82), respectively, using deionized water. Different versions of the seawater and low salinity brine solutions were prepared following previously published methods[25] **(Table 1)**. These synthetic brines were used for zeta potential analysis with the Indiana limestone rock samples. The chemical composition of the field-collected produced water samples is displayed in **Table 3**.

Table 2: Chemical composition of synthetic brine solution used.

Brine[a]	Ca^{2+}	Mg^{2+}	Na^{+}	K^{+}	Cl^{-}	SO_4^{2-}	IS[b], mol/L	TDS[c], ppm	pH
FWS	11000	2800	48000	500	101913	260	3.27	164473	5.71
SWS	2200	560	9600	100	20383	52	0.65	32895	6.03
SWS0S	2200	560	9640	100	20483	0	0.66	32983	6.40
SWS0Ca	0	560	13380	100	22320	52	0.65	36412	6.07
SWS0Mg	2200	0	11186	100	21195	52	0.65	34733	5.83
LSW	134	34	585	6	1243	3	0.04	2006	6.12
LSW0S	134	34	588	6	1249	0	0.04	2011	6.41
LSW0Ca	0	34	816	6	1361	3	0.04	2220	5.64
LSW0Mg	134	0	682	6	1292	3	0.04	2118	5.52

[a] Ion concentration in ppm. [b] ionic strength. [c] total dissolved solids

Table 3: Chemical composition of produced water samples.

Ion	**PW-1[a]**	**PW-2[a]**
K^{+}	76	75
Mg^{2+}	324	287
Sr^{2+}	63	64
Li^{+}	8	7
Ca^{2+}	1052	734
Na^{+}	6012	6406
Cl^{-}	12075	11766
SO_4^{2-}	1391	754
Br^{-}	50	37
NO_3^{-}	3	3
IS[b], mol/L	0.412	0.384
TDS[c], ppm	21053	20134
pH	7.11	7.11

[a] Ion concentration in ppm. [b] ionic strength. [c] total dissolved solids

2.3. Zeta Potential Measurement

Zeta potential measurements of the rock-brine interface were conducted using the electrophoresis mobility techniques offered by Brookhaven NanoBrook Omni Particle Size Analyzer. A Brookhaven BI-ZELF electrode was attached to the analyzer for the zeta potential measurement. The zeta potential was approximated using the Smoluchowski model [50], using a measurement procedure previously outlined in other publications [9, 25]. The pH of the filtered rock-brine colloidal solution was recorded before zeta potential measurement. The average of 3-5 measurements, with each measurement having 3 runs and 20 cycles, was presented as the rock-brine zeta potential. All the zeta potential values were measured at 25°C and under atmospheric CO_2 partial pressure of $10^{-3.4}$ atm. The measured rock-brine zeta potential was used

to fit the SCMs generated for the calcite-brine and the reservoir composite carbonate -brine interfaces. PW samples were chosen for the zeta potential analysis because they possessed brine salinity and composition similar to seawater typically used for low salinity waterflooding purposes in carbonate formations.

2.4. Model Development

2.4.1. DDL and TLM model description for pure calcite surfaces

In this section, a pure limestone surface was modeled by assuming a pure calcite surface with >CaOH and $>CO_3H$ as the primary hydration sites. Whole-charge chemical formulations (**Table 4**) for the calcite surface were employed in the development of both DDL and TLM based SCM. This approach is well established in the calcite literature [8, 30, 36, 58, 67, 68], and a similar approach has been employed to model the calcite-brine interface [36, 68]. Specific reaction constants for calcite sites, particularly, reactions for H^+ and OH^- association and dissociation, from surface calcite groups were adopted from works by Brady et al [8, 58]. Sorption constants for Ca^{2+} and Mg^{2+} association with carbonate sites were adopted from our previous works [9, 25,40], wherein experimental data were used to optimize these constants for calcite systems.

Figure 1 shows the schematic description of the SCM used to model pure calcite-brine interfaces. These hydration sites would protonate and deprotonate to form positive and negative reactive species, respectively. [8, 9, 12, 30, 51]. These reactive species would interact with the brine ions according to their chemical reactions and equilibrium sorption constants (**Table 4**). For the DDL model, the locations of the ions were not specified and hence assumed to interact with the calcite surface (X_o). The basic assumptions and equations related to the developed DDL in this section are similar to those used in our previous publications [9, 25, 40]. An approximation of the Poisson-Boltzmann equation to form the Debye-Hückel equation was used to estimate the zeta potential (see [9, 25] for details).

The TLM was simulated using the charge distribution, multi-site complexation model (CD-MUSIC) built into the PHREEQC geochemical software [26, 36, 52-54]. The net charge transferred from one plane to the next was modeled by assuming a ΔZ_i value for each plane (see **Table 4**) in the TLM [26, 36, 54].

However, oxyanion charges were not partially shared with the oxygen ions at the surface plane, following the approach used by Ding and Rahman [32] and Heberling et al. [33]. This ionic placement provided the best match to the experimental zeta potential. The three planes were assumed to act as a parallel plate with capacitance (C) inversely related to the distance between each plate. Different approaches have been used to define the C values for each plane. Elakneswaran and coworkers [36, 54, 68] determined the C values by using the diameter of the largest ion in each plane as inversely proportional to the C.Sø et al [69] varied the C_1 value between 1.3 to 3 F/m^2 and fixed C_2 at 4.5 F/m^2, which resulted in no significant change in the adsorption on the calcite surface. These C1 values corresponded to a plane thickness of 2.32 and 2.72 Å, which is within the range of the stern layer thickness (≤ 2.8 Å). In the TLM-based SCM, the surface charge density in the diffused layer (σ_{DL}) was computed from the Gouy-Chapman equation as:

$$\sigma_{DL} = -0.1174 I^{0.5} \sinh\left(\frac{F\psi_2}{2RT}\right) \qquad \textit{Equation 1}$$

where F is Faraday's constant, R is the universal gas constant, and T is the absolute temperature. The TLM assumed a linear drop for the potential at each plane based on the capacitance value used to calculate the potential and charge densities as shown below [41]:

$$\sigma_0 = C_1(\psi_o - \psi_1) \qquad \textit{Equation 2}$$

$$\sigma_0 + \sigma_1 = C_2(\psi_1 - \psi_2) \qquad \textit{Equation 3}$$

where σ_i and ψ_i represent the charge density (C/m^2) and the potential (mV), respectively, at plane *i*. For the TLM, the potential at the 0-plane (ψ_o) corresponds to the surface potential, while the potential at the 2-plane (ψ_2) could be directly compared to the zeta potential (ζ) [41, 54]. For the current work, C_1 and C_2 values are fixed at 1.3 F/m^2 and 4.5 F/m^2, respectively, similar to values reported in the literature [26, 27, 69], provided the best fit to experimental zeta potential measurements for the limestone rock and were used for the TLM models.

The DDL-and the TLM-based SCMs were evaluated against both experimentally measured zeta potential values in our previous publications [9, 25] and data from the literature [32, 55, 56]. For the calcite surface, a specific surface area of 1 m^2/g [32] and equilibration with atmospheric CO_2, i.e., partial pressure of $10^{-3.4}$ atm, was used for all predictions. A calcite site density of 4.95 sites/nm^2 [57] was assumed for the predictions unless otherwise stated. All predictions were performed at 25°C to match PHREEQC calculations with experimental conditions.

Table 4: Surface complexation reactions and equilibrium constants used for the DDL and TLM-based SCMs.

Calcite-brine		Surface reactions	ΔZ_0*	ΔZ_1*	Log (K) at 25°C
			TLM assumes these constants		
Calcium sites	1	$>CaOH + H^+ \leftrightarrow >CaOH_2^+$	1	0	11.85[a]
	2	$>CaOH_2^+ + SO_4^{2-} \leftrightarrow >CaSO_4^- + H_2O$	0	-2	2.1[a]
	3	$>CaOH + HCO_3^- \leftrightarrow >CaCO_3^- + H_2O$	0	-2	5.8[a]
Carbonate sites	4	$>CO_3H \leftrightarrow >CO_3^- + H^+$	-1	0	-5.1[a]
	5	$>CO_3H + Ca^{2+} \leftrightarrow >CO_3Ca^+ + H^+$	-1	2	-4.4[b]
	6	$>CO_3H + Mg^{2+} \leftrightarrow >CO_3Mg^+ + H^+$	-1	2	-4.4[b]

*represents the charge distribution values used for the dissociation and adsorption reactions at the calcite surface for the TLM. These values are not used for the DDL model since the ions are assumed to interact with the calcite surface at the stern layer.
[a] Referenced from Brady et al 2012 [58]
[b] Referenced from Tetteh et al 2020 [9]

2.4.2. Extended DDL and TLM model description for composite carbonate surfaces

Mineralogical analysis was performed, and the LKC reservoir carbonate rock was comprised of significant amounts of calcite, dolomite, and quartz minerals (Figure A1 and Table 1). Loss on ignition test performed on the powdered LKC carbonate rock showed 0.23% OM content. Thus, extended SCMs were developed, incorporating dolomite, quartz, and OM along with calcite mineral to form the composite carbonate surfaces representative of reservoir carbonate rock (**Figure 2**). Quartz and dolomite surfaces were

represented by >SiOH and >MgOH hydration sites (Table 5). The incorporation of each inorganic mineral was modeled by modifying the surface site density (SSD) for each primary reactive species based on a mass-law expression. Specific reaction constants for the dolomite and quartz sites were obtained from [63] and [58], respectively. Dolomite and quartz surface sites were assumed to replace calcite sites in proportion to their weight composition in the overall material.

OM in the form of carboxylic acid was incorporated in the model (Table 6) following the approach of Zeng et al. [62], who considered the OM to behave similarly to crude oil molecules. Specific reaction constants for OM were obtained from the same source [62]. The OM coverage, which was calculated as a percentage of the SSD of carbonate surface, was assumed to be present on the composite carbonate surface, increasing the total number of available sites. The total SSD of the composite carbonate with organic matter present was calculated as 4.962 sites/nm^2. By employing this approach, other minerals such as kaolinite and anhydrite that are present in some composite carbonate rocks could be included by incoporating their surface reactive sites into the total surface area of the rock surface. For the extended SCM work, the same C_1 and C_2 values (1.3 F/m^2 and 4.5 F/m^2, respectively) used for the pure calcite surface were employed. This assumes that, while the surface impurities will affect the overall electrokinetic properties of the composite carbonate surface, the calcite mineral would remain the dominant contributor.

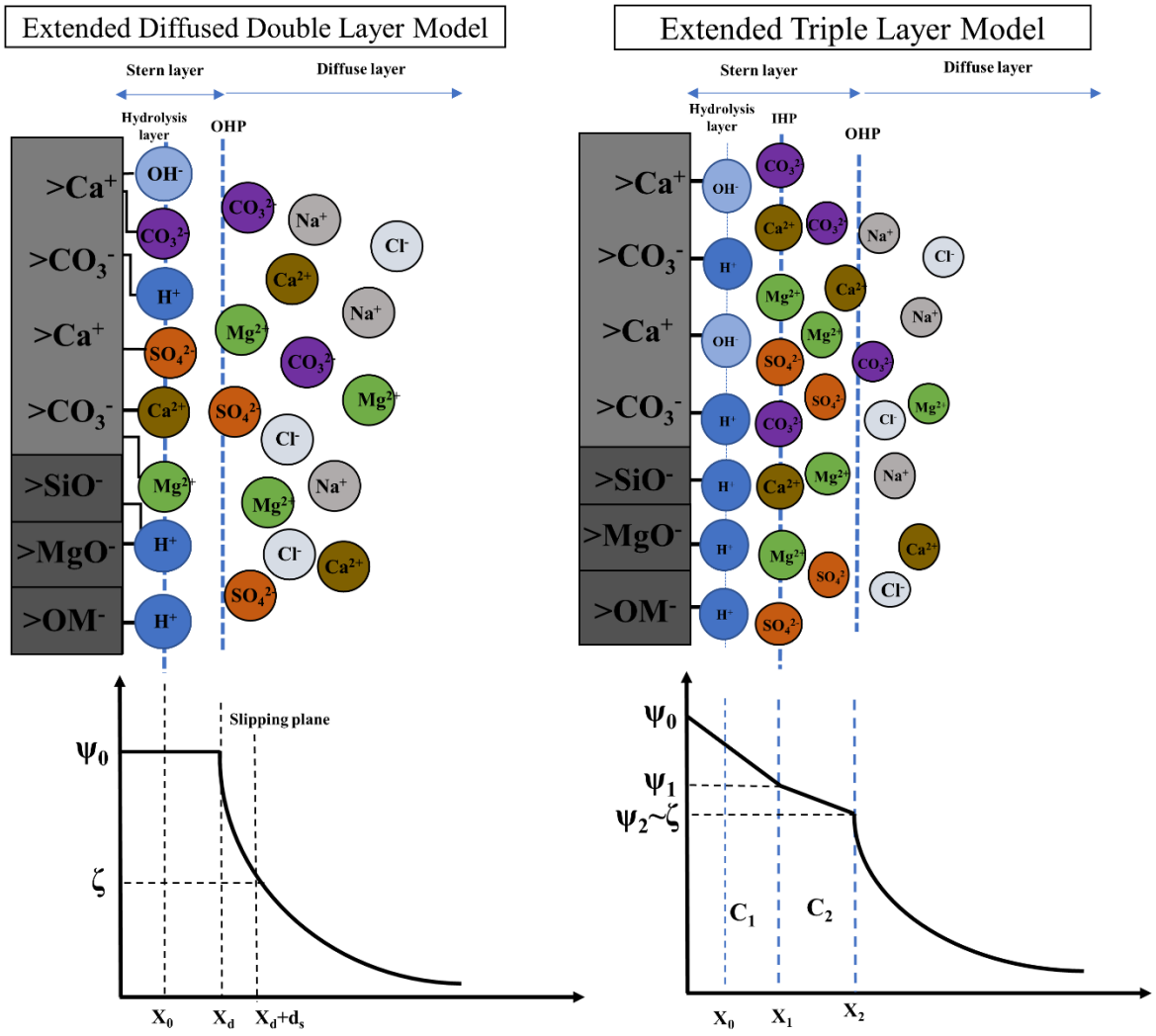

Figure 2: Schematic description of the extended diffused double layer (DDL) model (on the left) and the extended triple layer model (TLM, on the right) of a composite carbonate surface. Dolomite and quartz minerals and organic matter were included on the composite carbonate surface.

Table 5: Surface complexation reactions and equilibrium constants included to form the extended DDL and TLM-based SCMs.

Rock-brine**		**Surface reactions**	**ΔZ_0***	**ΔZ_1***	**Log (K) at 25°C**
			TLM assumes these constants		
Dolomite sites (0.579 sites/nm^2)	7	>MgOH ↔ MgO$^-$ + H$^+$	-1	0	-12[c]
	8	>MgOH + H$^+$ ↔ MgOH$_2^+$	1	0	10.4[c]

	9	$>MgOH + H^+ + CO_3^{2-} \leftrightarrow >MgCO_3^- + H_2O$	0	-2	15.4[c]
Quartz (0.168 sites/nm^2)	10	$>SiOH \leftrightarrow SiO^- + H^+$	-1	0	-7.0[a]
Organic matter (0.012 sites/nm^2)	11	$>OM\text{-}H \leftrightarrow >OM^- + H^+$	-1	0	-5.0[d]

[*]represents the charge distribution values used for the dissociation and adsorption reactions at the composite carbonate surface for the extended TLM. These values are not used for the extended DDL model since the ions are assumed to interact directly with the composite carbonate surface.
[**]Rock-brine interface for the extended SCM includes reactions 1-6 from **Table 4** with the calcite SSD adjusted to 4.202 sites/nm^2, which represents 84.9% calcite composition on the composite carbonate surface
[a] Referenced from Brady et al. 2012 [58]
[c] Referenced from Shabani and Zivar [63]
[d] Referenced from Zeng et al. [62]

3. Results and discussion

3.1. Effect of brine ionic strength on zeta potential predictions at the pure calcite-brine interface

Figure 3 shows the predictions of zeta potential measurement from Tetteh et al. [9] and Collini et al. [55] on outcrop limestone with ≥99% calcite composition and with brine ionic strength up to about 3.27 mol/L. Collini et al. [55] measured the zeta potential of the rock surface using the streaming potential technique by performing a single-phase coreflooding on the outcrop limestone rock. Thus, the exposed surface area to the brine injected would be lower than using the electrophoresis technique, which makes use of rock powder. Therefore, the surface site density was modified to 0.45 sites/nm^2, which fitted the zeta potential data measured through the streaming potential technique. The TLM-based SCM performed better in predicting the zeta potential of the outcrop limestone as a function of ionic strength. Table A1 in the supporting documents shows the root mean square error (RMSE) for the model evaluation, indicating the performance of both SCMs. For example, the TLM-based SCM had a RMSE of 2.08, as compared to 6.55 for the DDL model, when evaluating data from the work of Tetteh et al. [9]. In particular, TLM better matches the high ionic strength zeta potential values from Tetteh et al. [9]. Nevertheless, both models reflect the overall trends in zeta potential, which is paramount to the understanding of the low salinity waterflooding process. As brine ionic strength decreased into the range of low salinity brines (ionic strength

below 0.1 M), the calcite-brine zeta potential became negative and would generate a repulsive force at the crude oil-brine-rock (COBR) interface, improving oil recovery.

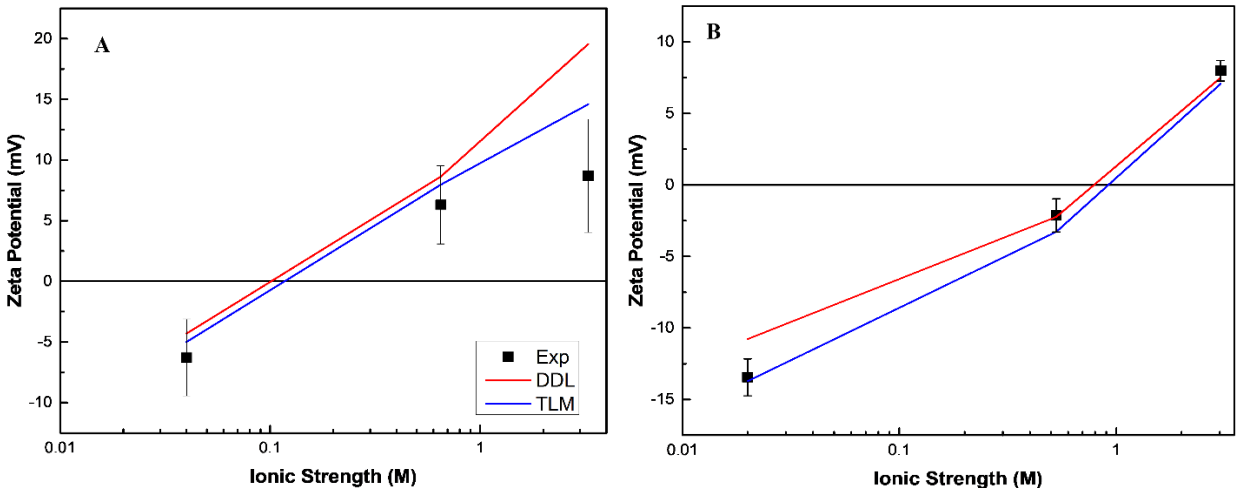

Figure 3: Effect of brine ionic strength on zeta potential prediction using the DDL and TLM- based SCM for experimental data from A) Tetteh et al [9] and B) Collini et al [55] at 25°C. Data from Collini et al. and outcrop rock TE with calcite composition of >99% was assumed for the SCM calculations, with brine composition borrowed from [55].

To fully explore the differences between the DDL and the TLM-based SCMs, surface charge density (SCD) and surface potential (SP) calculations as a function of ionic strength were determined based on experimental data from Tetteh et al. [9] (**Figure 4**). The SCD was proportional to the sum product of the species concentration and the charge of the species at the surface. The species concentration would be dependent on the placement of the ions in different planes in each SCM. The DDL-based SCM assumes ion placement on the calcite surface, while the TLM-based SCM spreads the ions across multiple planes in the calcite lattice. Thus, the concentration of the ions on the surface would differ for both SCM, resulting in different SCD values. The SCD for the DDL-based SCM was calculated to be positive at an ionic strength of 3.27 mol/L, but decreased significantly from 0.127 C/m^2 to –0.0027 C/m^2 as ionic strength reduced to 0.04 mol/L. The TLM-based SCM, on the other hand, predicted only a slight decrease in SCD because of the spatial distribution of the ions onto the calcite lattice. The DDL-based SCM also predicted a consistently higher SP than the TLM-based SCM. The calculations of zeta potential from the SP values were also different for both SCMs. While the DDL-based SCM model assumes an exponential decay based on the expression for the distance of the slipping plane (the Debye Hückle approximation [9]) , the TLM-based

SCM assumes a capacitance between two plane to define the distance of the shear plane (assumed to coincide with the slipping plane). Thus, each model provides a different prediction of the zeta potential. The TLM-based SCM considers the influence of the electrolyte ions through their spatial placement on the different planes, thus making the sorption constants independent of electrolyte concentration [59]. This effect makes the TLM based SCM a better model for predicting zeta potential, SCD, and SP at higher ionic strength than the DDL-based SCM.

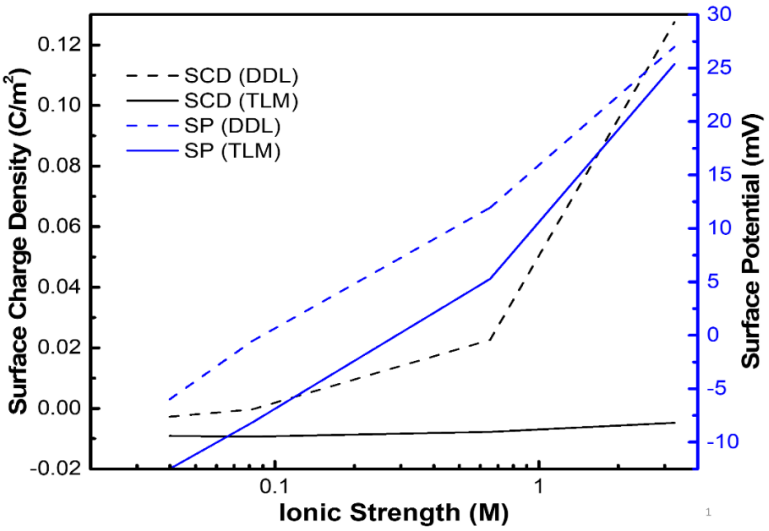

Figure 4: Effect of ionic strength on surface charge density and surface potential prediction from the DDL and TLM-based SCMs for the calcite-brine interface using rock and brines from Tetteh et al. [9].

The SCD and the SP were calculated based on the surface concentrations of the charged species. These species are important to understanding the role of electrostatic interactions towards destabilizing the water film at the COBR interface, which causes rock wettability alterations [8, 9, 58]. For instance, the $>CaOH_2^+$ and $>CO_3^-$ species are known to interact with the carboxylic acid ($-COO^-$) and the amine ($-NH^+$) species of the oil-brine interface, forming $[>CaOH_2^+][-COO^-]$ and $[>CO_3^-][-NH^+]$ electrostatic bonds, respectively. These two bonds dominate electrostatic attractions at the COBR interface with the greatest impact on calcite wettability [8, 9, 30, 37]. An increase in the electrostatic bond strength of $[>CaOH_2^+][-COO^-]$ and $[>CO_3^-][-NH^+]$ would shift the rock surface wettability towards oil wetness, while a decrease would shift wettability towards water-wetness. Thus, their accurate predictions would improve the understanding of the

wettability alteration process associated with modified salinity waterflooding. The TLM-based SCM predicted lower concentrations for the positive species (>$CaOH_2^+$, >CO_3Ca^+, >CO_3Mg^+) and higher concentrations for the negative species (>CO_3^-, >$CaCO_3^-$ and >$CaSO_4^-$) at higher ionic strength when compared to the DDL-based SCM (**Figure 5** also see **Table 6** for changes in species concentration). This resulted in the TLM-based SCM predicting lower SCD and SP and hence a lower zeta potential at high ionic strength as compared to the DDL-based SCM, which better matches the experimental data in **Figure 3**. At low ionic strength, both models made similar speciation predictions. As brine ionic strength reduced, the concentration of the dominant >CO_3^- species increased more sharply than the >$CaOH_2^+$ species, hence shifting the zeta potential towards negative polarity. The concentration of the >$CaSO_4^-$ and >CO_3Mg^+ would balance out because of their similar concentrations, opposite polarity, and trends with respect to decreasing ionic strength at the calcite surface. Therefore, the reduction in the >CO_3Ca^+ and the increase in >$CaCO_3^-$ species concentration with decreasing ionic strength would both contribute towards the negative SCD, SP, and hence the negative zeta potential predicted using both SCMs.

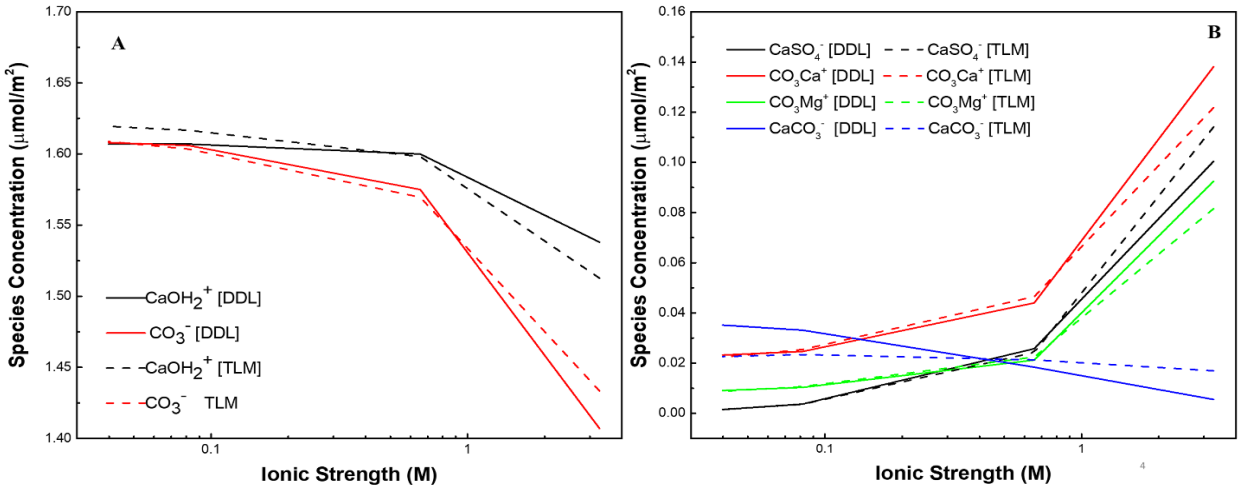

Figure 5: Effect of ionic strength on surface concentration of reaction species formed on the calcite surface using both DDL and TLM-based SCMs. Brine and rock composition from Tetteh et al. [9].

3.2. Effect of brine ionic composition on zeta potential predictions at the pure calcite-brine interface

Models were used to calculated zeta potential and compared to data from Ding and Rahman [32], Alroudhan et al. [56], and Tetteh et al. [25] for different brine compositions (**Figure 6**). It should be noted

that the results presented in **Figure 6** were from different sources with slightly different rock materials, brine composition, and experimental procedure. Ding and Rahman [32] used Iceland spar calcite (~98% calcite), Alroudhan et al. [56] used Portland outcrop limestone (~97% calcite), and Tetteh et al. [25] used Indiana limestone (~99% calcite). All materials were modeled as pure calcite. For the zeta potential predictions by Alroudhan et al. [56], calcite site density of 0.45 sites/nm^2 was again used because the streaming potential technique was employed to measure the calcite-brine zeta potential. Ding and Rahman [32] and Tetteh et al. [25] both employed the electrophoresis technique in the zeta potential measurement. In general, both DDL and TLM-based SCMs performed well in predicting the zeta potential trends at the calcite-brine interface; however, the predictions show some noticeable differences. The TLM-based SCM predicted a higher magnitude of zeta potential as compared to the DDL-based SCM for **Figure 6A and B**. Both SCMs performed comparably with an RMSE of 5.68 and 5.36 for DDL and TLM-based SCMs, respectively for data from Tetteh et al. [25](**Figure 6**C). The DDL-based SCM predicted a more negative zeta potential for the mixed ionic compositions brine in **Figure 6**D when compared to the TLM-based SCM. Thus, the observation of different trends for the SCMs showed that the placement of ions in different planes for the TLM has an effect on the predicted electrokinetic properties as compared to placing all ions on the calcite surface for the DDL-based SCM.

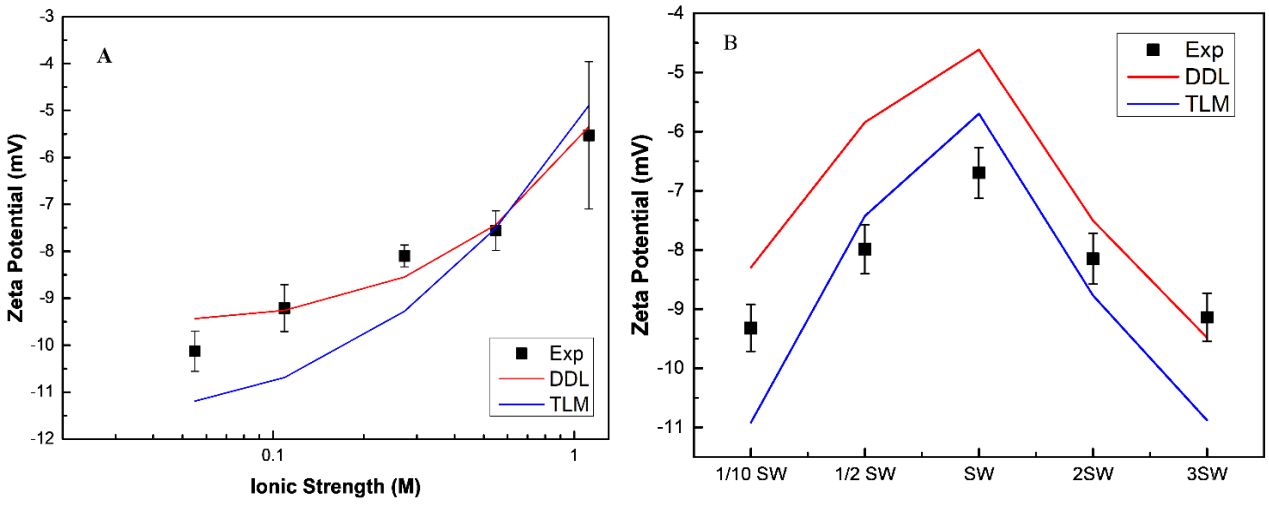

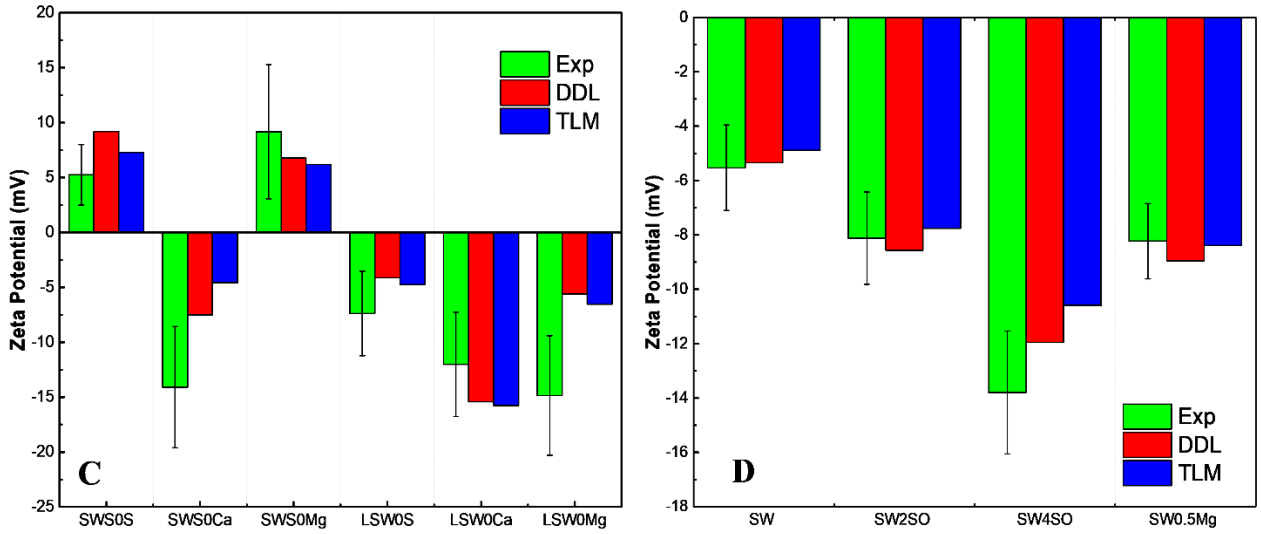

Figure 6: Effect of ionic composition on zeta potential prediction using the DDL and TLM- based SCM for experimental data from A) Ding and Rahman [32] using diluted seawater brine, B) Alroudhan et al. [56], C) Tetteh et al. [25], and D) Ding and Rahman [32], using seawater brine with modified concentration of PDIs all at 25°C. Iceland spar calcite Portland limestone (outcrop)and Indiana limestone (outcrop) were used for zeta potential measurement for Ding and Rahman [32], Alroudhan et al [56], Tetteh et al [25], respectively. Brine composition used can be found in the references therein.

The surface electrokinetic properties of the calcite-brine interface studied by Ding and Rahman [32] (**Figure 6**A and D) were further explored by predicting the SCD and the SP. TLM-based SCM predicted higher SCD and lower SP for the calcite-brine interface compared to the DDL-based SCM across all ionic strengths (**Figure 7**A). Increasing ionic strength reduced the calculated SCD for both SCMs but resulted in an increase in SP predicted by both models. Again, the change in SCD with ionic strength was insignificant for the TLM-based SCM. Increasing the SO_4^2 concentration resulted in a decrease in the SP at the calcite-brine interface using both SCMs (**Figure 7**B) and explains the observed decrease in zeta potential (i.e. zeta potential becomes more negative) at the calcite-brine interface as SO_4^{2-} concentration increases. The TLM-based SCM consistently predicted a lower SP at the calcite brine interface than the DDL-based SCM across all conditions (**Figure 7**). The difference in the predicted SCD and SP is attributed to the use of a constant capacitance model approximation for the Gouy Chapman equation in the DDL-based SCM as compared to the different capacitance used for each plane in the TLM-based SCM.

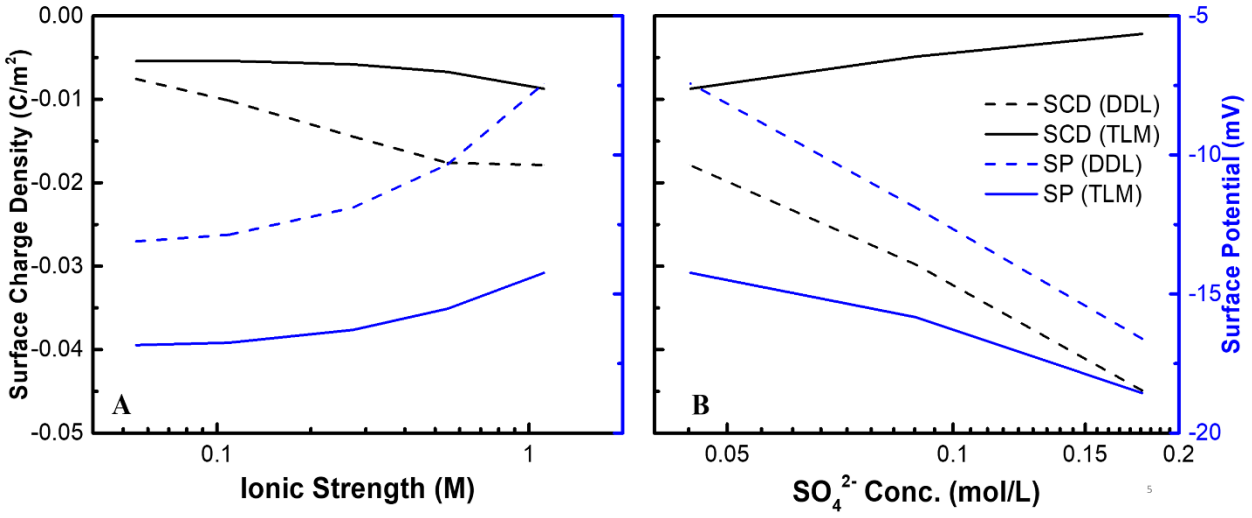

Figure 7: Effect of A) ionic strength and B) SO_4^{2-} concentration on surface charge density and surface potential prediction from the DDL and TLM-based SCMs for the calcite-brine interface using rock and brines from Ding and Rahman [32].

The increase in $>CaOH_2^+$ concentration and decrease in $>CO_3^-$ species, from the DDL to TLM-based SCMs (**Figure 8**B and **Table 6**) would make the SCD less negative at the calcite-brine interface for TLM-based SCM (**Figure 7**B). In both SCMs, the increase in $>CO_3Mg^+$ and $>CaSO_4^-$ species was accompanied by a decrease in the $>CaOH_2^+$ and $>CO_3^-$ species, which would lessen electrostatic strength of the $[>CaOH_2^+][-COO^-]$ and $[>CO_3^-][-NH^+]$ bonds and shift the wettability state on calcite surfaces towards more water wetness. $>CO_3Mg^+$ species have a greater influence on the electrokinetic surface properties than the $>CO_3Ca^+$ species, mainly due to the higher concentration of Mg^{2+} (2110 ppm) than Ca^{2+} (650 ppm) in the brine solution used. $>CaCO_3^-$ concentrations on the calcite surface are low using both SCM, and thus have less impact on the electrokinetic properties. Nonetheless, the TLM-based SCM predicted a lower $>CaCO_3^-$ concentration than the DDL-based SCM, highlighting the effect of ionic placement for reaction 3 in **Table 4**.

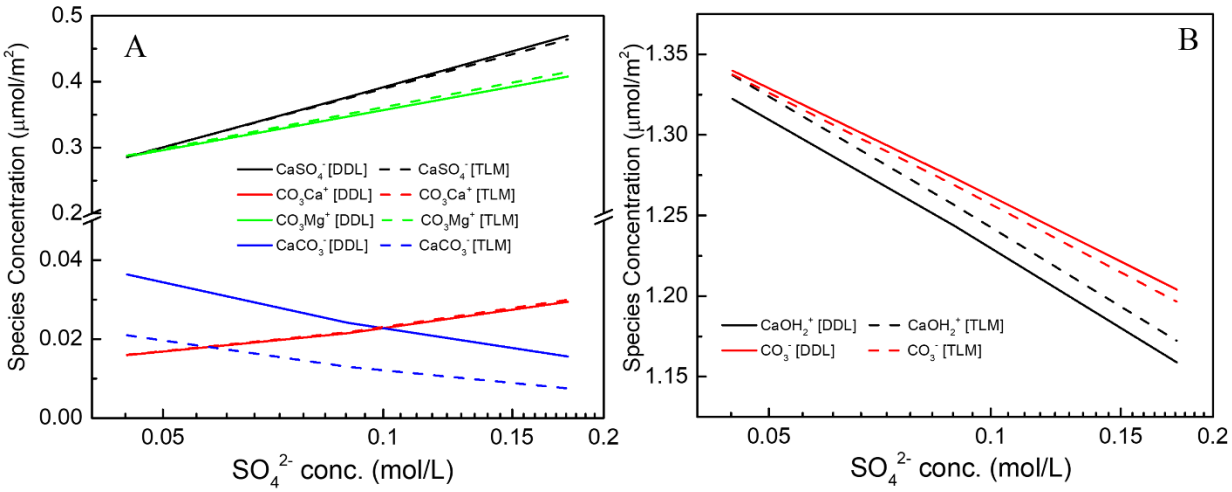

Figure 8: Effect of SO_4^{2-} concentration on surface species formed on the calcite surface using the both DDL and TLM-based SCMs. Seawater brine with increasing SO_4^{2-} and rock composition from Ding and Rahman [32] was used for the calculation.

Table 6: Relative changes in species concentration on calcite surfaces between SCMs.

	Higher ionic strength (~3M)	Effect of SO_4^{2-}
$>CaOH_2^+$	↓	↑
$>CO_3^-$	↑	↓
$>CO_3Ca^+$	↓	-
$>CO_3Mg^+$	↓	↑
$>CaSO_4^-$	↑	↓

Note: ↑ and ↓ represents an increase and decrease, respectively, in species concentration from the DDL-based SCM to the TLM-based SCM, where "–" represents no apparent change in species concentration

3.3. Predicting electrokinetic properties for reservoir composite carbonate surfaces

In investigating the low salinity waterflooding process, outcrop limestone rock or synthetic calcite powder are usually used to measure the zeta potential of the calcite-brine interface when exposed to modified salinity and composition brines [22, 31, 48, 60]. However, these surrogate rocks do not provide a complete picture of the role of electrokinetics in determining the wettability of the rock surface since reservoir carbonate rocks contain other inorganic minerals (quartz, dolomite, anhydrite, etc.) and OM impurities. These rocks could be considered composite carbonates due to the high proportion of the other inorganic minerals. Both the organic and inorganic components in composite carbonate surfaces are reactive and can influence the measured zeta potential of the limestone-brine interface [61]. These phenomena have been observed in naturally occurring and reservoir carbonate surfaces that return a greater

magnitude of negative zeta potential than synthetically pure calcite surfaces [22-24]. Therefore, the next step was to measure zeta potential and predict the electrokinetic properties for a reservoir composite carbonate surface.

The previously developed SCMs were used to match the experimentally measured zeta potential using two PW samples (PW-1 and PW-2) in **Figure 9**. Both SCMs captured the zeta potential trends and provided a reasonable fit to the zeta potential data of the rock-brine interface (See Table A1 for RMSE for model evaluation). However, the magnitude of predicted zeta potential shifted slightly from the measured values. As previously indicated, the current SCMs ignore the contribution of different mineralogical compositions and the organic matter coverage of actual reservoir composite carbonate rocks. This section explores the effect of these inorganic and organic components incorporated onto composite carbonate surface on the electrokinetic properties and carbonate wettability.

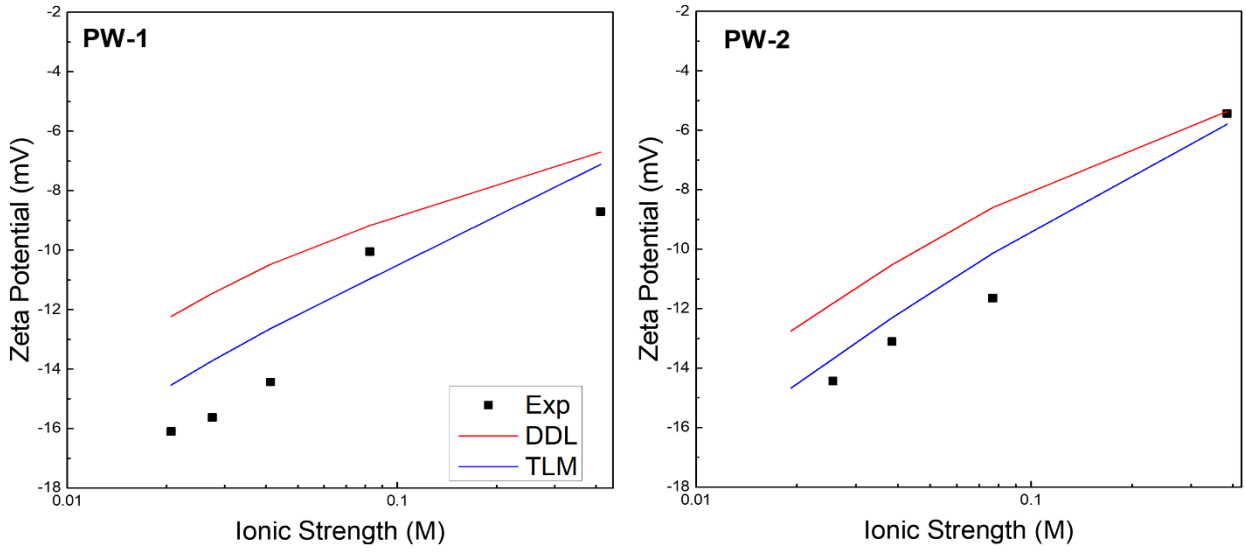

Figure 9: Zeta potential prediction using the DDL and TLM- based SCM for experimental data using reservoir LKC limestone rock and produced water samples. The current SCMs cannot accurately capture the measured zeta potential values, hence an adjustment is needed.

The extended TLM-based SCM captured the trends and closely matched measured zeta potential values using both PW samples, while the extended DDL-based SCM model captured the general trends but underestimated the magnitude of the measured zeta potential (**Figure 10**). The RMSE for model evaluation improved from 1.6 to 1.4 for PW-1 and from 1.6 to 0.7 for PW-2 using the extended TLM-based SCM

(Table A1). Thus, the TLM-based SCM better represents the impact of inorganic minerals and OM coverage present when predicting the electrokinetic properties of composite carbonate surfaces. The deficiency in the extended DDL-based SCM in predicting the zeta potential magnitude could be attributed to two simplifying assumptions in the model. First, the assumption of a constant capacitance from the Gouy Chapman approximation ignores the relative position of the ions in appropriate planes that would influence the interface. Thus, the inclusion of new reactions assumed to be occurring at the composite carbonate surface would significantly impact the electrokinetic surface properties. Second, the Debye Hückel approximation was developed for 1:1 symmetrical electrolyte solution and could result in inaccuracies for the PW sample used. [46, 47].

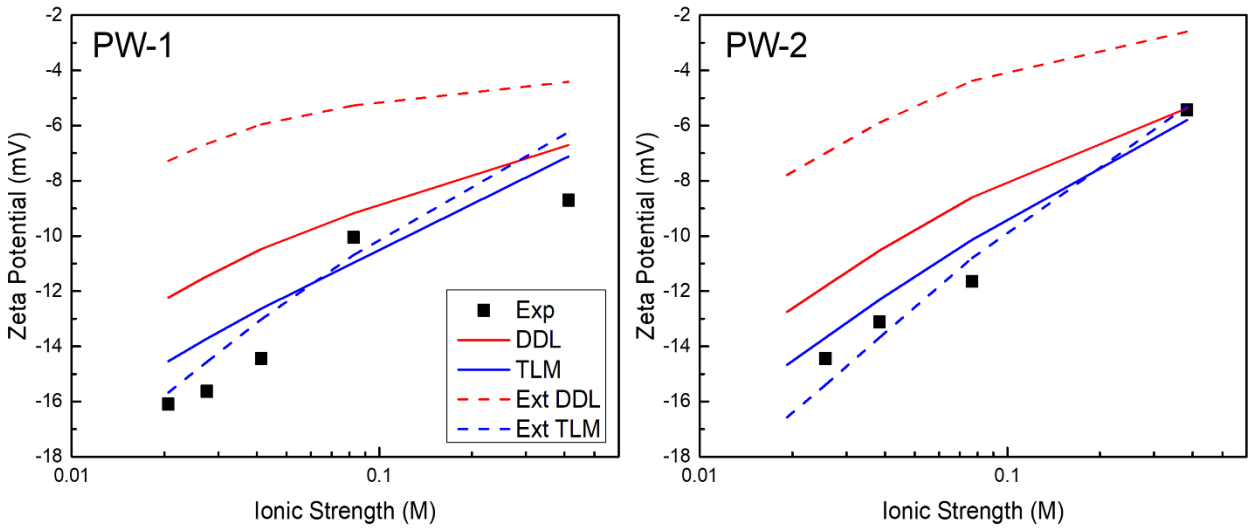

Figure 10: Comparison of zeta potential prediction using the extended DDL and TLM-based SCM for experimental data using reservoir LKC carbonate rock and produced water samples. The extended DDL-based SCM failed to capture the measured zeta potential, while the extended TLM-based SCM slightly improves the prediction of the measured zeta potential over the initial TLM-based SCM.

Incorporating the impurities onto the electrokinetic models impacted the species concentration associated with the calcite surface (**Figure 11**). The inclusion of the impurities reduced the total site density of the primary hydration sites of calcite and hence consistently decreased the concentration of the calcite primary species ($>CaOH_2^+$ and $>CO_3^-$) as indicated in **Figure 11**A. Similarly, the concentration of Mg^{2+} and Ca^{2+} ions associated with the calcite surface decreased when the SCM was extended to include the impurities also due to the lower site density for the calcite hydration sites (**Figure 11**B). The extended DDL also predicted higher SO_4^{2-} adsorption onto the composite carbonate surface, although the extended TLM model indicated the opposite effect (**Figure 11B)**. Thus, the inclusion of the reactions associated with the

impurities (reactions 7-11) impacts surface species concentrations, affecting the overall electrokinetic surface properties and shifting the predicted zeta potential, as indicated in **Figure 10**.

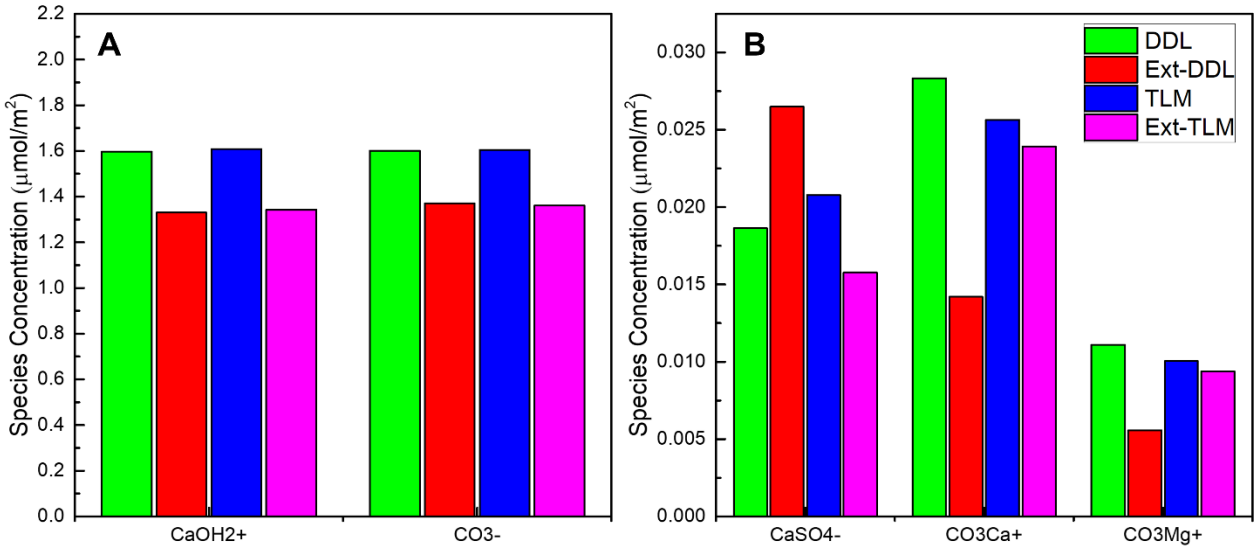

Figure 11: Effect of impurities (extended SCM) on the species concentration as compared to pure calcite surface using diluted PW-1 brine with ionic strength of 0.02 M at an initial pH of 7.1.

The extended TLM-based SCM consistently predicted higher and lower concentrations for the positive ($>CaOH_2^+$, $>CO_3Ca^+$, $>CO_3Mg^+$) and negative ($>CO_3^-$ and $>CaSO_4^-$) calcite-related species, respectively, as compared to the extended DDL-based SCM (**Figure 12**A and B). However, opposite trends were observed at the dolomite and quartz surfaces. The extended TLM-based SCM predicted higher concentration for the negative quartz surface species ($>SiO^-$) and lower concentration for the positive dolomite surface species ($>MgOH_2^+$) than the extended DDL-based SCM (**Figure 12**C). It should also be noted that the four new reactions associated with the protonation and deprotonation of the reactive species of the inorganic minerals and OM coverage were placed in the IHP (0-plane) for the TLM based SCM. Reaction 9 was placed on OHP (1-plane) in the TLM-based SCM. The DDL-based SCM placed all five new reactions on the IHP (0-plane), which correspond to the composite carbonate surface. The biggest changes in species concentration were associated with $>CaOH_2^+$ and $>CO_3^-$, which signified the increased emphasis on the protonation and deprotonation reactions at the 0-plane (**Figure 12**). $>MgOH_2^+$ was the dominant species amongst the impurities incorporated onto the composite carbonate surface. Thus, although

the dolomite associated species were observed to be non-reactive with respect to ionic strength due to the high sorption constants, their contribution towards the electrokinetic surface properties would be higher than the other impurities. A summary of the relative changes in the species concentration from the extended DDL-based SCM to the TLM-based SCM is provided in **Table 7**.

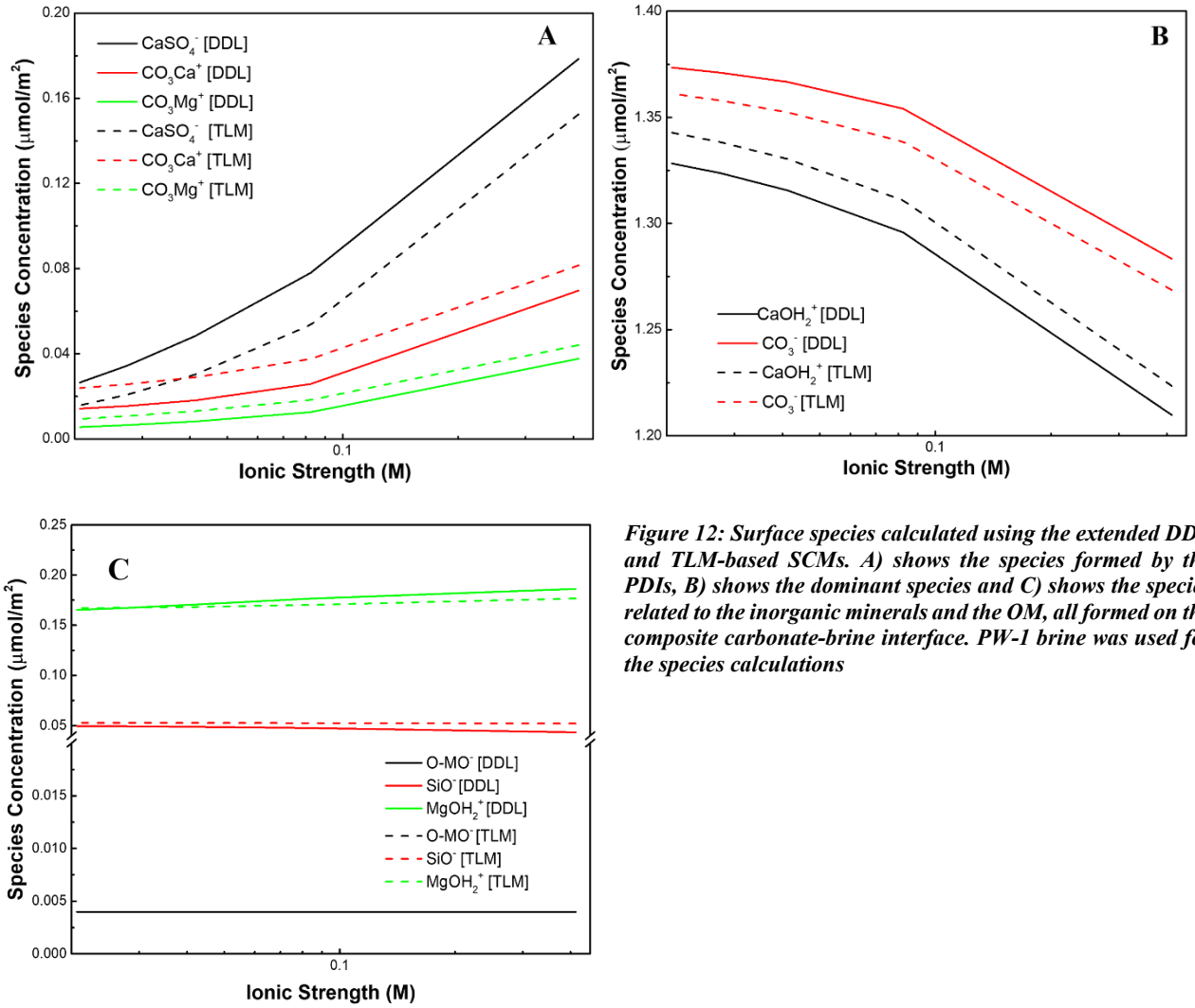

Figure 12: Surface species calculated using the extended DDL and TLM-based SCMs. A) shows the species formed by the PDIs, B) shows the dominant species and C) shows the species related to the inorganic minerals and the OM, all formed on the composite carbonate-brine interface. PW-1 brine was used for the species calculations

Greater changes in concentration of the calcite-related species and the higher magnitude of other species predicted by extended TLM-based SCM yielded a positive polarity for the surface properties (**Figure 13**). These results are contrary to the extended DDL-based SCM that predicted negative polarities (**Figure 13**). Thus, the prediction of negative zeta potential by the extended TLM could be attributed to the effect of the different capacitance values (Equation 2 and 3). The difference between positive and negative polarity for

the surface properties could be very important in analyzing the wettability state of rock surfaces. The crude oil-brine interface has been observed to exhibit negative surface potential due to the dominance of carboxylic acid [5, 9]. The surface potential on the rock-brine surface would determine the thermodynamic stability of the water film influencing the surface wettability. The same polarity at both crude oil-brine and rock-brine interface would develop a repulsive disjoining pressure, making the water film to be thicker and stable, hence increasing water wetness. Opposite polarity at both interfaces would develop an attractive disjoining pressure, collapsing the water film and making the rock surface more oil-wet [1, 4, 9]. Reservoir composite carbonate rocks have been known to exhibit more oil wetness after aging compared to the outcrop carbonate rocks. In contact angle measurement performed by Treiber and Owens [64] on about 25 reservoir carbonate rocks, 84% of the carbonate surfaces were observed to be oil-wet, 8% were observed to be intermediate wet, and the remaining 8% were observed to be water-wet. However, Graue et al. [65] observed that the wettability state of 50 outcrop carbonate rocks was mainly intermediate wet using Amott Wettability Index. Thus, the observed oil-wet surface condition of reservoir carbonate rocks is more consistent with a positive surface potential; an effect only captured using the TLM based SCM. The positive SP predicted by the TLM-based SCM, would generate attractive electrostatic forces with negatively charged crude oil surfaces [6, 66] resulting in an oil-wet surface. This phenomenon makes it very important to accurately capture the electrokinetic surface properties of reservoir composite carbonate surfaces, as seen with the extended TLM-based SCM.

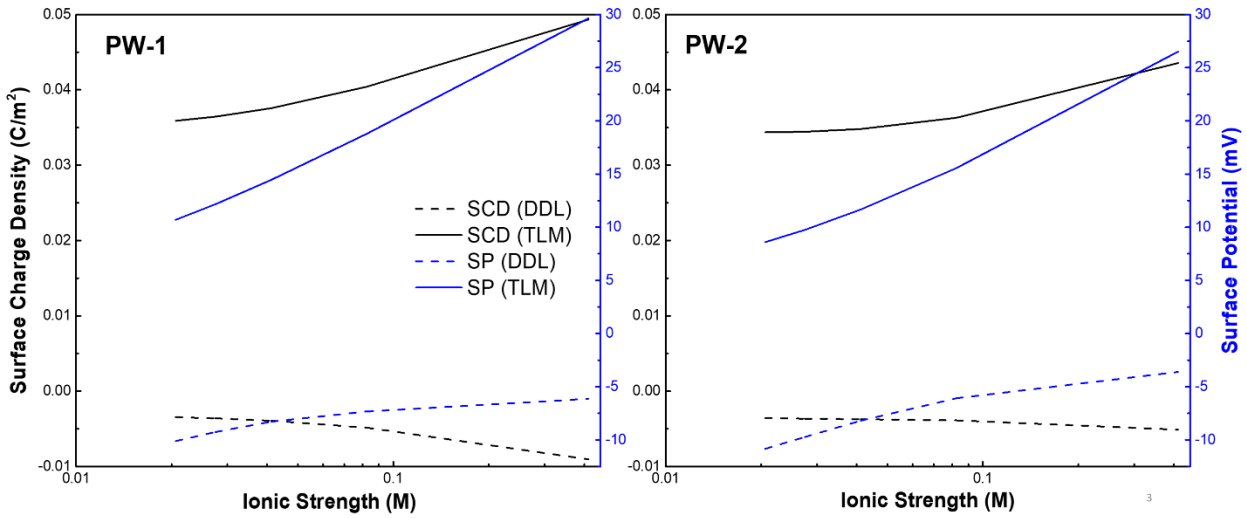

Figure 13: Surface charge density (SCD) and surface potential (SP) prediction from the extended DDL and TLM-based SCMs of composite carbonate surface interaction with PW samples.

Table 7: Relative changes in species concentration on composite carbonate surfaces between SCMs. ↑ and ↓ represents an increase and decrease, respectively, in surface species concentration from the extended DDL-based SCM to the TLM-based SCM. – represents no apparent change in species concentration

	Relative changes
$>CaOH_2^+$	↑
$>CO_3^-$	↓
$>CO_3Ca^+$	↑
$>CO_3Mg^+$	↑
$>CaSO_4^-$	↓
$>SiO^-$	↑
$>MgOH_2^+$	↓
$>OM^-$	-

4. Conclusions

In this work, electrokinetic properties on a rock surface were characterized by developing four different SCMs. The first two models were DDL and TLM-based SCMs that assumed a pure calcite-brine interface in fitting zeta potential. These SCMs were used to model the outcrop carbonate surfaces in brines with ionic strength up to ~3M. Ionic placements at different planes in the stern layer, as modeled by the TLM-based SCM, better matched experimental data at high ionic strength (~3.27 M) due to its independence from brine

ionic concentration. The DDL-based SCM assumed ionic interaction directly with the calcite surfaces and a constant capacitance theory; hence the role of ionic strength greatly impacts the double layer stability.

Extended versions of both the DDL and TLM-based SCMs were developed to predict zeta potential for reservoir composite carbonate surface in contact with PW samples. A mass-law expression was used to incorporate the contribution of non-calcite mineral components (dolomite and quartz) and organic matter into the overall model. The extended TLM-based SCM better predicted the trends and magnitude of the measured zeta potential from experimental data, while the extended DDL-based SCM only captured the zeta potential trends. Opposite SCD and SP polarities were predicted by the two modeling approaches: positive SCD and SP for the extended TLM-based SCM and negative SCD and SP for the extended DDL-based SCM. The differences in predicting the electrokinetic surface properties are attributed to the competitive protonation and deprotonation reactions placed at the 0-plane for the TLM-based SCM, hence having the greatest impact at the rock surface. $>MgOH_2^+$ species from the dolomite were observed to have the greatest impact on the electrokinetic surface properties amongst the modeled non-calcite components. The extended TLM-based SCM thus may provide an explanation for the observed oil-wet nature of reservoir carbonate rocks with varying mineral composition. This work has highlighted the importance of the accurate placement of ions at the appropriate planes related to colloidal rock surfaces, particularly for high salinity solutions, and has correctly represented reservoir carbonate rock surface for electrokinetic characterization useful for wettability classifications.

Acknowledgements

The authors are grateful to National Science Foundation EPSCoR Research Infrastructure Improvement Program: Track -2 Focused EPSCoR Collaboration award (OIA- 1632892) and the Kansas Water Resources Institute for their partial financial support of this project. The authors would also like to acknowledge the American Chemical Society Petroleum Research Funds (award number 59031-ND9) for partially funding this project. The authors would also like to thank Bryan Javier Rodriguez-Colon for help with the XRD data acquisition and analysis. The authors appreciate the work by K-State Soil Testing Lab for the loss of

ignition test on the reservoir carbonate samples used in this work. Tertiary Oil Recovery Program (TORP) labs are acknowledged for providing analytical resources related to analysis of water and rock samples.

References

[1] Tetteh JT, Brady PV, Ghahfarokhi RB. Review of low salinity waterflooding in carbonate rocks: mechanisms, investigation techniques, and future directions. Advances in Colloid and Interface Science 2020:102253.

[2] Alotaibi MB, Cha D, Alsofi AM, Yousef AA. Dynamic interactions of inorganic species at carbonate/brine interfaces: An electrokinetic study. Colloids and Surfaces A: Physicochemical and Engineering Aspects 2018;550:222-35.

[3] Afekare DA, Radonjic M. From Mineral Surfaces and Coreflood Experiments to Reservoir Implementations: Comprehensive Review of Low-Salinity Water Flooding (LSWF). Energy & Fuels 2017;31(12):13043-62.

[4] Guo H, Nazari N, Esmaeilzadeh S, Kovscek AR. A Critical Review of the Role of Thin Liquid Films for Modified Salinity Brine Recovery Processes. Current Opinion in Colloid and Interface Science 2020;50:101393.

[5] Buckley JS, Takamura K, Morrow NR. Influence of Electrical Surface Charges on the Wetting Properties of Crude Oils. SPE Reservoir Engineering 1989;4:332-40.

[6] Buckley JS, Liu Y, Monsterleet S. Mechanisms of Wetting Alteration by Crude Oils. SPE Journal 1998;3:54-61.

[7] Kovscek AR, Wong H, Radke CJ. A pore-level scenario for the development of mixed wettability in oil reservoirs. AIChE Journal 1993;39:1072-85.

[8] Brady PV, Thyne G. Functional Wettability in Carbonate Reservoirs. Energy and Fuels 2016;30:9217-25.

[9] Tetteh JT, Alimoradi S, Brady PV, Barati Ghahfarokhi R. Electrokinetics at calcite-rich limestone surface: Understanding the role of ions in modified salinity waterflooding. Journal of Molecular Liquids 2020;297:111868.

[10] Jackson MD, Al-Mahrouqi D, Vinogradov J. Zeta potential in oil-water-carbonate systems and its impact on oil recovery during controlled salinity water-flooding. Scientific Reports 2016;6:37363.

[11] Mahani H, Keya AL, Berg S, Bartels WB, Nasralla R, Rossen WR. Insights into the mechanism of wettability alteration by low-salinity flooding (LSF) in carbonates. Energy and Fuels 2015;29.

[12] Mahani H, Keya AL, Berg S, Nasralla R. Electrokinetics of Carbonate/Brine Interface in Low-Salinity Waterflooding: Effect of Brine Salinity, Composition, Rock Type, and pH on zeta-potential and a Surface-Complexation Model. SPE Journal 2017;22:053-68.

[13] Mahani H, Menezes R, Berg S, Fadili A, Nasralla R, Voskov D, et al. Insights into the Impact of Temperature on the Wettability Alteration by Low Salinity in Carbonate Rocks. Energy and Fuels 2017;31:7839-53.

[14] Song J, Wang Q, Shaik I, Puerto M, Bikkina P, Aichele C, et al. Effect of salinity, Mg2+ and SO42− on “smart water”-induced carbonate wettability alteration in a model oil system. Journal of Colloid and Interface Science 2020;563:145-55.

[15] Austad T, Shariatpanahi SF, Strand S, Aksulu H, Puntervold T. Low Salinity EOR Effects in Limestone Reservoir Cores Containing Anhydrite: A Discussion of the Chemical Mechanism. Energy and Fuels 2015;29:6903-11.

[16] Austad T. Water Based EOR in Carbonates and Sandstones : New Chemical Understanding of the EOR-Potential Using “ Smart Water ”. Enhanced Oil Recovery Field Cases 2013:301-32.

[17] Zhang P, Austad T. Wettability and oil recovery from carbonates: Effects of temperature and potential determining ions. Colloids and Surfaces A: Physicochemical and Engineering Aspects 2006;279:179-87.

[18] Zhang P, Tweheyo MT, Austad T. Wettability alteration and improved oil recovery in chalk: The effect of calcium in the presence of sulfate. Energy and Fuels 2006;20:2056-62.
[19] Zhang P, Tweheyo MT, Austad T. Wettability alteration and improved oil recovery by spontaneous imbibition of seawater into chalk : Impact of the potential determining ions Ca 2 + , Mg 2 + , and SO 42 −. 2007;301:199-208.
[20] Rezaeidoust A, Puntervold T, Strand S, Austad T. Smart water as wettability modifier in carbonate and sandstone: A discussion of similarities/differences in the chemical mechanisms. Energy and Fuels 2009;23:4479-85.
[21] Purswani P, Tawfik MS, Karpyn ZT. Factors and Mechanisms Governing Wettability Alteration by Chemically Tuned Waterflooding: A Review. Energy & Fuels 2017;31:7734-45.
[22] Song J, Hirasaki GJ, Biswal SL, Rezaee S, Vargas F, Puerto M, et al. Characterizing the Influence of Organic Carboxylic Acids and Inorganic Silica Impurities on the Surface Charge of Natural Carbonates Using an Extended Surface Complexation Model. Energy & Fuels 2019.
[23] Vdović N. Electrokinetic behaviour of calcite - The relation with other calcite properties. Chemical Geology 2001;177:241-8.
[24] Vdović N, Bišćan J. Electrokinetics of natural and synthetic calcite suspensions. Colloids and Surfaces A: Physicochemical and Engineering Aspects 1998;137(1-3):7-14.
[25] Tetteh JT, Veisi M, Brady PV, Barati Ghahfarokhi R. Surface Reactivity Analysis of the Crude Oil–Brine–Limestone Interface for a Comprehensive Understanding of the Low-Salinity Waterflooding Mechanism. Energy & Fuels 2020:acs.energyfuels.9b03664.
[26] Bonto M, Eftekhari AA, Nick HM. A wettability indicator parameter based on the thermodynamic modelling of chalk-oil-brine systems. Energy & Fuels 2020.
[27] Taheriotaghsara M, Bonto M, Nick HM, AkbarEftekhari A. Estimation of calcite wettability using surface forces. Journal of Industrial and Engineering Chemistry 2021.
[28] Chen Y, Xie Q, Pu W, Saeedi A. Drivers of pH increase and implications for low salinity effect in sandstone. Fuel 2018;218:112-7.
[29] Chen Y, Ubaidah A, Elakneswaran Y, Niasar VJ, Xie Q. Detecting pH and Ca2+ increase during low salinity waterflooding in carbonate reservoirs: Implications for wettability alteration process. Journal of Molecular Liquids 2020;317:114003.
[30] Chen Y, Xie Q, Sari A, Brady PV, Saeedi A. Oil/water/rock wettability: Influencing factors and implications for low salinity water flooding in carbonate reservoirs. Fuel 2018;215:171-7.
[31] Song J, Zeng Y, Wang L, Duan X, Puerto M, Chapman WG, et al. Surface complexation modeling of calcite zeta potential measurements in brines with mixed potential determining ions (Ca2+, CO32−, Mg2+, SO42−) for characterizing carbonate wettability. Journal of Colloid and Interface Science 2017;506:169-79.
[32] Ding H, Rahman SR. Investigation of the Impact of Potential Determining Ions from Surface Complexation Modeling. Energy & Fuels 2018;32:9314-21.
[33] Heberling F, Eng P, Lützenkirchen J, Trainor TP, Bosbach D, Denecke MA. Structure and reactivity of the calcite–water interface. Journal of Colloid and Interface Science 2010;354:843-57.
[34] Heberling F, Bosbach D, Eckhardt JD, Fischer U, Glowacky J, Haist M, et al. Reactivity of the calcite-water-interface, from molecular scale processes to geochemical engineering. Applied Geochemistry 2014;45:158-90.
[35] Yousef AA, Al-Saleh SH, Al-Kaabi A, Al-Jawfi MS. Laboratory Investigation of the Impact of Injection-Water Salinity and Ionic Content on Oil Recovery From Carbonate Reservoirs. SPE Reservoir Evaluation & Engineering 2011;14:578-93.
[36] Takeya M, Ubaidah A, Shimokawara M, Okano H, Nawa T, Elakneswaran Y. Crude oil/brine/rock interface in low salinity waterflooding: Experiments, triple-layer surface complexation model, and DLVO theory. Journal of Petroleum Science and Engineering 2020;188:106913.
[37] Erzuah S, Fjelde I, Omekeh AV. Wettability Estimation Using Surface-Complexation Simulations. SPE Reservoir Evaluation & Engineering 2018:12-5.

[38] Kasha A, Al-Hashim H, Abdallah W, Taherian R, Sauerer B. Effect of Ca2+, Mg2+ and SO42− ions on the zeta potential of calcite and dolomite particles aged with stearic acid. Colloids and Surfaces A: Physicochemical and Engineering Aspects 2015;482:290-9.
[39] Hiorth A, Cathles LM, Madland MV. The Impact of Pore Water Chemistry on Carbonate Surface Charge and Oil Wettability. Transport in Porous Media 2010;85:1-21.
[40] Tetteh JT, Brady PV, Barati Ghahfarokhi R. Impact of temperature and SO42- on electrostatic controls over carbonate wettability. Colloids and Surfaces A: Physicochemical and Engineering Aspects 2021;625:126893.
[41] Ding H. Investigating the Effects of Ca 2 + , Mg 2 + and SO 42- on the Wettability of Carbonate Rocks. *School of Petroleum Engineering.* University of New South Wales; 2019.
[42] Goldberg S. Adsorption Models Incorporated into Chemical Equilibrium Models. Chemical Equilibrium and Reaction Models. 1995, p. 75-95.
[43] Goldberg S, Criscenti LJ, Turner DR, Davis JA, Cantrell KJ. Adsorption–Desorption Processes in Subsurface Reactive Transport Modeling. Vadose Zone Journal 2007;6(3):407-35.
[44] Stipp SLS. Toward a conceptual model of the calcite surface: Hydration, hydrolysis, and surface potential. Geochimica et Cosmochimica Acta 1999;63:3121-31.
[45] Al Mahrouqi D, Vinogradov J, Jackson MD. Zeta potential of artificial and natural calcite in aqueous solution. Advances in Colloid and Interface Science 2017;240:60-76.
[46] Appelo CAJ, Postma D. Geochemistry, Groundwater and Pollution. 2005;59.
[47] Israelachvili JN. Intermolecular and Surface Forces. Elsevier 2011;3rd:1-30.
[48] Ding H, Mettu S, Rahman SS. Impacts of Smart Waters on Calcite-Crude Oil Interactions Quantified by "soft Tip" Atomic Force Microscopy (AFM) and Surface Complexation Modeling (SCM). Industrial and Engineering Chemistry Research 2020.
[49] Tetteh JT, Barati R. Crude-Oil/Brine Interaction as a Recovery Mechanism for Low-Salinity Waterflooding of Carbonate Reservoirs. SPE Reservoir Evaluation & Engineering 2019;22:0877-96.
[50] Weiner B, Zhang Y. How to choose a zeta potential ánalyzer : general guidelines. 2014;1:1-7.
[51] Brady PV, Krumhansl JL. A surface complexation model of oil–brine–sandstone interfaces at 100°C: Low salinity waterflooding. Journal of Petroleum Science and Engineering 2012;81:171-6.
[52] Hiemstra T, Van Riemsdijk WH. A Surface Structural Approach to Ion Adsorption: The Charge Distribution (CD) Model. Journal of Colloid and Interface Science 1996;179:488-508.
[53] Parkhurst DL, Appelo CAJ. Description of input and examples for PHREEQC Version 3 — A computer program for speciation, batch-reaction, one-dimensional transport, and inverse geochemical calculations. US Geological Survey Techniques and Methods, book 6, chapter A43 2013:6-43A.
[54] Takeya M, Shimokawara M, Elakneswaran Y, Nawa T, Takahashi S. Predicting the electrokinetic properties of the crude oil/brine interface for enhanced oil recovery in low salinity water flooding. Fuel 2019;235:822-31.
[55] Collini H, Li S, Jackson MD, Agenet N, Rashid B, Couves J. Zeta potential in intact carbonates at reservoir conditions and its impact on oil recovery during controlled salinity waterflooding. Fuel 2020;266:116927.
[56] Alroudhan A, Vinogradov J, Jackson MD. Zeta potential of intact natural limestone: Impact of potential-determining ions Ca, Mg and SO4. Colloids and Surfaces A: Physicochemical and Engineering Aspects 2016;493:83-98.
[57] Wolthers M, Charlet L, Van Cappellen P. The surface chemistry of divalent metal carbonate minerals: A critical assessment of surface charge and potential data using the charge distribution multi-site ion complexation model. American Journal of Science 2008;308:905-41.
[58] Brady PV, Krumhansl JL, Mariner PE. Surface Complexation Modeling for Improved Oil Recovery. *SPE Improved Oil Recovery Symposium.* Society of Petroleum Engineers; 2012:14-8.
[59] Wen X, Du Q, Tang H. Surface Complexation Model for the Heavy Metal Adsorption on Natural Sediment. Environmental Science & Technology 1998;32(7):870-5.

[60] Lu Y, Najafabadi NF, Firoozabadi A. Effect of Temperature on Wettability of Oil/Brine/Rock Systems. Energy and Fuels 2017;31:4989-95.
[61] Mohammed I, Al Shehri DA, Mahmoud M, Kamal MS, Alade O. Surface Charge Investigation of Reservoir Rock Minerals. Energy & Fuels 2021;35(7):6003-21.
[62] Zeng L, Chen Y, Hossain MM, Saeedi A, Xie Q. Wettability alteration induced water uptake in shale oil reservoirs: A geochemical interpretation for oil-brine-OM interaction during hydraulic fracturing. International Journal of Coal Geology 2019;213:103277.
[63] Shabani A, Zivar D. Detailed analysis of the brine-rock interactions during low salinity water injection by a coupled geochemical-transport model. Chemical Geology 2020;537:119484.
[64] Treiber LE, Owens WW. A Laboratory Evaluation of the Wettability of Fifty Oil-Producing Reservoirs. Society of Petroleum Engineers Journal 1972;12:531-40.
[65] Graue A, Viksund BG, Eilertsen T, Moe R. Systematic wettability alteration by aging sandstone and carbonate rock in crude oil. Journal of Petroleum Science and Engineering 1999;24(2):85-97.
[66] Hirasaki GJ. Wettability: Fundamentals and Surface Forces. SPE Formation Evaluation 1991;6:217-26.
[67] Lützenkirchen J. Comparison of 1-pK and 2-pK Versions of Surface Complexation Theory by the Goodness of Fit in Describing Surface Charge Data of (Hydr)oxides. Environ Sci Technol 1998;32:3149–54. https://doi.org/10.1021/es980125s.
[68] Hao X, Abu-Al-Saud M, Ayirala S, Elakneswaran Y. Influence of carbonate impurities on smartwatereffect: Evaluation of wettability alteration process by geochemical simulation. J Mol Liq 2021;340:117165. https://doi.org/https://doi.org/10.1016/j.molliq.2021.117165.
[69] Sø HU, Postma D, Jakobsen R, Larsen F. Competitive adsorption of arsenate and phosphate onto calcite; experimental results and modeling with CCM and CD-MUSIC. Geochim Cosmochim Acta 2012;93:1–13. https://doi.org/10.1016/j.gca.2012.06.021

Predicting the Electrokinetic Properties on an Outcrop and Reservoir Composite Carbonate Surfaces in Modified Salinity Brines using Extended Surface Complexation Models

Joel T. Tetteh[1,2*], Anthony Pham[2], Edward Peltier[2], Justin M. Hutchison,[2] and Reza Barati Ghahfarokhi[1,3]

[1]Chemical and Petroleum Engineering Department, University of Kansas

[2]Civil, Environmental, and Architectural Engineering Department, University of Kansas

[3]Tertiary Oil Recovery Project, University of Kansas

[*]Correspondence to: Joel T. Tetteh (Email: joelteyetetteh@gmail.com)

Supporting Information

This supporting document shows the thin section analysis indicating the presence of non-calcite minerals and impurities associated with the LKC rock, hence influencing the electrokinetic properties. We also showed the root square mean error for the model fitting to the experimentally measured zeta potential values.

Thin section image illustrates the clean grainstone texture, and no clay content (either as matrix or in stylolites) for Indiana limestones (Figure A1 left). The predominant grain types are skeletal grains and ooids with intra-particle and inter-particle pores, some of which are occluded by equant calcite cement. For the LKC cores, the pores were lined with some non-calcite components with grain types of skeletal and ooids grains. The pore structure was mainly inter-particle and intra-particle with a few moldic pores (Figure A1 right). The thin section images supported the XRD analysis, with Indiana showing pure calcite nature, while LKC showed mixed mineralogical composition. Also, the surface coverage of LKC pore with non-calcite minerology supports the assertion that pure calcite surfaced SCM would not accurately capture electrostatic interactions associated with reservoir limestone pore surfaces

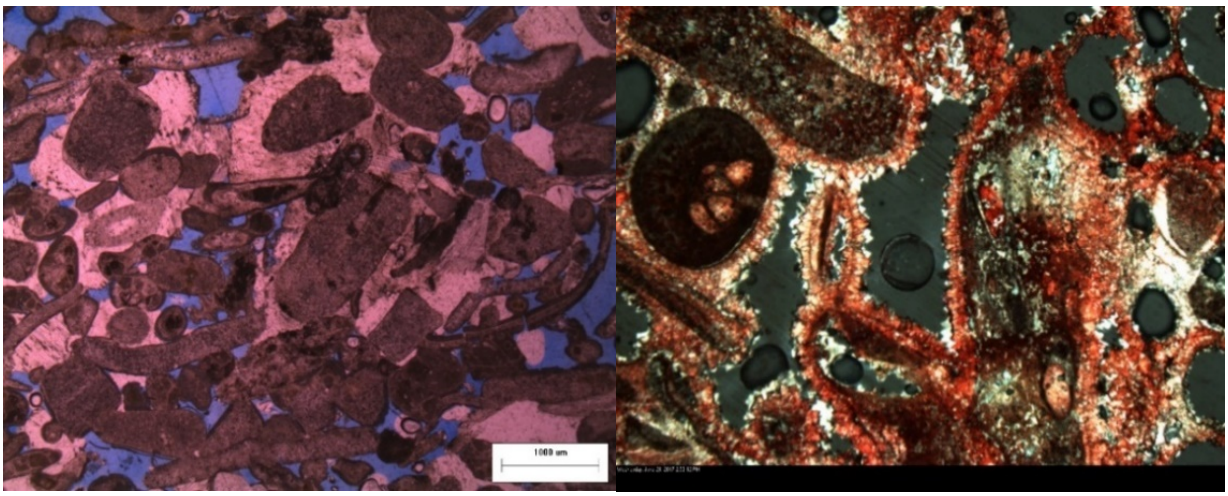

Figure A1: Petrographic thin section images of Indiana Limestone (Left) and LKC limestone (Right). Thin section pores are indicated with blue epoxy with rock consisting of calcitic oolitic grainstone.

Table A1: Root mean square error (RMSE) calculated for the model predictions of the SCMs

	DDL	TLM	Figure	Comments
Tetteh et al [9]	6.51	2.08	Figure 2A	
Collini et al [55]	0.74	0.22	Figure 2B	
Ding et al [32]	0.38	1.01	Figure 5A	
Alroudhan et al. [56],	1.45	1.21	Figure 5B	
Tetteh et al [25]	5.37	5.68	Figure 5C	

Ding et al [32]	1.02	1.65	Figure 5D	
PW-1	3.25	1.59	Figure 8	SCM for Pure Calcite surface
PW-2	3.25	1.59	Figure 8	SCM for Pure Calcite surface
PW-1	7.37	1.40	Figure 10	Extended SCM for limestone surface
PW-2	6.49	0.70	Figure 10	Extended SCM for limestone surface

1